Impulsive Noise Mitigation with Interleaving Based on MUSIC in Power Line Communication

Article *in* IEEE Transactions on Smart Grid · April 2018

DOI: 10.1109/TSG.2018.2831913

3 authors, including:

Li Bai
Università di Pisa

Mauro Tucci
Università di Pisa

Impulsive Noise Mitigation with Interleaving Based on MUSIC in Power Line Communication

Li Bai, Mauro Tucci, *Member, IEEE* and Marco Raugi

***Abstract*—In power line communication (PLC), impulsive noise (IN) greatly degrades the performance of signal transmission. Generally, IN model adopts Middleton Class A or Bernoulli Gaussian model, with the assumption that IN is sparse and memoryless. However, IN collected in fields appears in bursts. In this paper, interleaving in time domain is applied to create a special structure in frequency domain for IN burst. Based on the special structure, IN support is determined by using multiple signal classification (MUSIC) and its amplitude is estimated by Least Squares (LS) method in frequency domain, exploiting the noise information on null subcarriers in orthogonal frequency division multiplexing (OFDM) system. In addition, sparse Bayesian Learning algorithm with IN support based on MUSIC is also investigated. Simulations are conducted to evaluate the proposed IN estimation performance, with varying ratio of IN power to background noise power (INR), and number of null subcarriers.**

***Index Terms*—impulse noise mitigation, MUSIC, interleaving, SBL, power line communication.**

I. INTRODUCTION

POWER line communications (PLC), is currently considered as an attractive communication system in smart grid because of its ubiquitous infrastructure and low-cost operation maintenance. It can be applied in automatic meter reading (AMR), demand side response, real-time monitoring and vehicle charging in smart grid [1]. However, power line is designed for transmitting power instead of high frequency band signals such as up to 30MHz or higher. Power line channels suffer from multipath and frequency-selective fading caused by diverse topologies and impedance mismatch [2] and noise interferences mainly generated by all the connected electrical devices [3].

Power line noise can be classified into five types including colored background noise, narrowband interferences and periodic IN asynchronous to the mains, periodic IN synchronous to the mains and asynchronous IN [4]. In power line communication, multicarrier modulation of orthogonal frequency division multiplexing (OFDM) is adopted to combat inter-symbol interferences and fading caused by multipath and narrowband interference [5]. However, asynchronous IN is of short-time duration and high amplitude, causing wide bandwidth occupation up to 11MHz in frequency domain, which degrades the quality of signal transmission [3].

To combat IN, many investigations have been done for years. Time domain interleaving, frequency domain interleaving and hybrid methods were proposed to spread IN onto longer time window and wider frequency bandwidth to combat IN [6]-[9]. Besides, block channel coding also was applied to mitigate the effects of IN by introducing redundancy [10]-[11]. These methods above are applied at transceiver without reducing any power of IN. They are dedicated to suppressing impulsive noise with low occurrence and amplitude, but they cannot perform well in the occasions of high occurrence and amplitude.

Therefore, impulsive noise reduction and mitigation methods were proposed. Nonlinear methods, including clipping, blanking, and combined clipping and blanking [12]-[13] were proposed to limit IN, without giving a closed expression of the thresholds for nonlinear processing. An adaptive threshold clipping was proposed based on computer searching [14]. A clipping method based on receiver operating characteristic with Bernoulli Gaussian (BG) modeled power line noise was proposed, in which threshold was estimated using moment estimation [15]. As a matter of fact, the optimal threshold strongly depends on the characteristics of IN. In previous publications, optimal threshold has been derived, given knowledge about the interference statistics. In general, however, no reliable information about the interference statistics is known at the receiver side. Adaptive blanking threshold was estimated based on the received signal without consideration of noise model, depending on the receiver samples [16]. The nonlinear method of combined clipping and blanking were further developed by introducing weights based on BG model [17], and blanking was further discussed in real-valued OFDM PLC systems [18]. Combined with nonlinear processing at receiver, preprocessing the transmitted signal at the transmitter was also applied to highlight IN at the receiver, which introduced unwanted distortions in the transmitted signal [19]-[20].

These nonlinear methods above attempt to seek an optimal threshold to diminish the power of IN, but they distort signal when limiting IN. Moreover, they require extra training overhead and suffer from performance degradation when the noise model or parameters are not in accordance with the possibly time varying noise statistics. To get rid of the demand of prior knowledge, the methods below attempt to recover IN by exploiting the sparse structure of IN in the time domain. The methods proposed in [21]-[24] applied compressive sensing (CS) techniques to estimate the IN from null subcarriers of the received signal. Sparse Bayesian learning (SBL) algorithm was applied to estimate IN from both null subcarriers and data subcarriers to improve performance and robustness, compared with CS [25]-[26]. However, CS and SBL algorithms demand expense computation even though they perform better than nonlinear methods. The special structure of sensing matrix,

L. Bai, M. Tucci, and M.Raugi are with the Department of Energy, Systems, Territory and Constructions Engineering, University of Pisa, Pisa, 56122, Italy e-mail: baili123246530@gmail.com

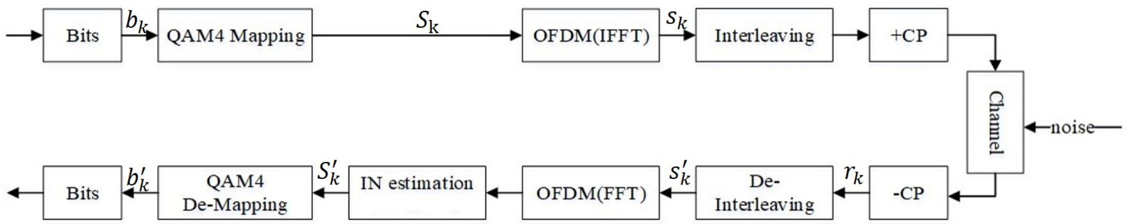

Fig. 1. OFDM PLC system diagram.

namely Fourier matrix, was explored to estimate IN supports, considering that IN occurrence probability follows binominal distribution in BG model, and IN amplitudes are estimated using minimum mean square error (MMSE) with the prior knowledge of IN power [27]. Compared with CS and SBL algorithms, the method proposed in [27] requires less complexity, while it depends too much on noise model. It needs the threshold of IN occurrence probability in the process of determining IN support, and prior knowledge of IN power in the process of noise amplitude estimation [27]. Multiple signal classification (MUSIC) method was applied to estimate the candidate supports of IN coarsely and then expand support into neighborhood locations, taking into account the effect brought by impulsive noise to background noise ratio (INR) and sample windows for estimation [28]-[29]. Besides, IN amplitudes were estimated identically using MMSE with prior knowledge of IN power as described in [27]. In [27]-[29], prior knowledge is still required at receiver, while it is difficult to know at receiver.

Regarding the complexity of the algorithms of SBL, CS and MMSE used in impulsive noise mitigation and assuming that the total number of all the subcarriers is N_{all} and that of null subcarriers is N_{null}, the complexity involved in each iteration of SBL based on the information of null subcarriers is $O(N_{null}^3 + N_{all}^2 N_{null})$ [25]. On the other hand, the algorithm with the lower complexity $O(N_{all} N_{null}^2)$ is matching pursuit, which is considered to have the same order complexity as smoothed L0 algorithm under CS framewok [30]. MMSE only involves matrix multiplication and inversion operation once. In addition, MUSIC used in this paper contains several matrix operations, including eigenvalue decomposition, to be performed only once.

In addition, noise models adopted in [17]-[18], [21]-[29] were Middleton Class A (MCA) model and simplified BG model, with the assumption that impulsive noise samples are scattered and independent in the time domain. However, IN measured in indoors environment occurs in bursts, presented in [3]- [4].

In our paper, a hidden Markov Middleton (HMM) model is adopted to characterize IN bursts instead of MCA model. To completely get rid of IN prior knowledge, we used an interleaving scheme to scatter IN bursts in the time domain, offering a special structure to recover IN. IN supports are estimated by MUSIC using only one parameter of background noise power, without any knowledge of IN occurrence probability distribution or INR. IN spectrum is firstly recovered in frequency domain by least square (LS) method, and then transformed into the time domain using fast Fourier transform (FFT). In addition, MUSIC with SBL based IN support is also elaborated to cut off computation overhead.

II. System Model

In power line communication, OFDM is adopted to combat narrowband interference and ISI. The diagram of OFDM PLC system is presented in Fig.1. At the transmitter, the generated bit stream b_k is mapped into complex symbols as S_k by quadrature amplitude modulation 4 (QAM4), and then modulated onto multiple carriers frequencies by OFDM technique. The transmitted signal s_k in the time domain is interleaved, and cyclic prefix (CP) is added before transmitting over power line channel. At the receiver, the received signal r_k is de-interleaved as $S_k^{'}$ after removing CP, and then demodulated into original transmitted symbol $s_k^{'}$, and finally it is de-mapped into bit stream $b_k^{'}$. IN is estimated and then mitigated from received signal. In our discussion, we mainly focus on the IN mitigation, assuming that power line channel is frequency flat for all the subcarriers.

Most of work regarding noise mitigation is based on MCA model or simplified Bernoulli Gaussian (BG) Model, assuming that IN is independent and sparsely scattered in the time domain. As a matter of fact, most of IN in the time domain occurs in bursts as observed in [3]-[4]. HMM Model was proposed to characterize the memory property of IN [31]. In our OFDM PLC system, HMM of two terms, namely hidden Markov BG model is applied. In addition, a complex system model is adopted that the transmitted signal and noise are generated in complex form.

The probability of distribution (PDF) of a real valued Class A noise n_k is given by

$$f(n_k) = \sum_{m=0}^{\infty} p_m N(n_k; 0, \delta_m^2), \tag{1}$$

where $N(n_k; 0, \delta_m^2)$ is Gaussian distribution with zero mean and its variance of δ_m^2, $p_m = \frac{e^{-A} A^m}{m!}$ and $\delta_m^2 = \delta_w^2(\frac{m}{A\Gamma} + 1)$. A is impulsive index and Γ is the ratio of background noise to IN. The truncated two-term MCA model refers to BG model, in which noise is composed of two terms: IN and background noise. The amplitude of IN is considered to follow a Gaussian process with zero-mean and its variance of δ_i^2, while the background noise adopts Gaussian distribution with zero-mean and variance δ_w^2. The noise sample n_k can be described as

$$n_k = i_k + w_k, \tag{2}$$

where i_k represents IN, and w_k represents background noise. Therefore, PDF of noise follows

$$p(n_k) = p_i^{'} N(n_k; 0, \delta_i^2 + \delta_w^2) + (1 - p_i^{'}) N(n_k; 0, \delta_w^2), \quad (3)$$

where $p_i^{'}$ denotes the normalized probability of IN occurrence and can be expressed as

$$p_i^{'} = \frac{A}{1 + A}. \quad (4)$$

In hidden Markov BG models, correlation index x is introduced to model the memory of IN. The hidden Markov BG model is illustrated Fig. 2. Its corresponding transition matrix is

$$T = \begin{bmatrix} x + (1-x)(1-p_i^{'}) & (1-x)p_i^{'} \\ (1-x)(1-p_i^{'}) & x + (1-x)p_i^{'} \end{bmatrix}.$$

In PLC system, OFDM technique is adopted. The received signal in the time domain r_k can be expressed as

$$r_k = s_k + i_k + w_k, \quad (5)$$

where s_k represents the desired signal, assuming that it follows a complex Gaussian distribution with zero-mean and its variance of δ_s^2. Given the noise variance, impulsive noise to background noise ration (INR) is defined as δ_i^2/δ_w^2, namely $1/\Gamma$, and signal to background noise ratio (SNR) is defined as δ_s^2/δ_w^2. In OFDM PLC systems, the received signal in the frequency domain can be modeled as

$$R = Fs + Fi + Fw = Fs + I + W, \quad (6)$$

in which F is FFT matrix, I and W are impulsive noise and background noise in the frequency domain respectively. In fact, not all the subcarriers are used for signal transmission in the frequency domain. Here unused subcarriers, referred to null subcarriers, contain no information of desired signal but that of noise. On null subcarriers, the model in the frequency domain is shown as

$$R_{null} = I_{null} + W_{null} = F_{null} i + W_{null}, \quad (7)$$

where subscript $()_{null}$ represents submatrix of the received signal on null subcarriers.

With IN estimation $\hat{i}$ in the time domain described in the following sections, IN can be canceled from the received signal, and the remained signal $\hat{r}$ can be expressed as

$$\hat{r} = s + (i - \hat{i}) + w. \quad (8)$$

III. Interleaving

A. Special Structure of Pseudo-Noise Sequence

According to [27], we design a PN sequence of length J oversampled with an equalized interval M in the time domain, where both M and J are powers of 2, and $N = JM$. The general form of the sequence in the time domain is denoted as row vector x^α in (9). In the expression of x^α, we define

$$\tilde{x}^\alpha = \begin{bmatrix} \tilde{x}_0^\alpha & \tilde{x}_1^\alpha & \cdots & \tilde{x}_{J-1}^\alpha \end{bmatrix}. \quad (10)$$

All J elements in $\tilde{x}^\alpha$ are separated by $M^{'}$ zeros, except that α zeros and $M^{'} - \alpha$ zeros at the start and end, with $M^{'} = M - 1$ and $0 \le \alpha \le M - 1$. The N points of the Fourier transform of x^α will be denoted as X^α in the frequency domain, and the J points of the Fourier transform of $\tilde{x}^\alpha$ will be denoted as $\tilde{X}^\alpha$ in the frequency domain. X^α has M segments with J elements in each segment. X^α can be expressed as

$$X^\alpha(J\tilde{m} + \tilde{j}) = \tilde{X}^\alpha(\tilde{j}) e^{-i\frac{2\pi\tilde{j}\alpha}{N}} e^{-i\frac{2\pi\tilde{m}\alpha}{M}}, \quad (11)$$

where $0 \le \tilde{m} \le M - 1$, $0 \le \tilde{j} \le J - 1$. From (11), the relationship between each two segments is

$$X^\alpha(\tilde{m}_1) = X^\alpha(\tilde{m}_2) e^{-i\frac{2\pi(\tilde{m}_1 - \tilde{m}_2)\alpha}{M}}, \quad (12)$$

where $X^\alpha(\tilde{m}_1)$ and $X^\alpha(\tilde{m}_2)$ are the $\tilde{m}_1$th and $\tilde{m}_2$th segment in the frequency domain. If one segment and α are given in advance, all the other segments can be calculated based on (12).

B. Interleaving with Pseudo-noise Sequence

In an OFDM symbol, interleaving in the time domain is applied to spread the impulsive noise into a wider band, in order to combat IN. At the receiver, de-interleaving is the inverse process of interleaving for recovering the original transmitted signal, and it interleaves IN as well. Based on the special structure described in Section III A, we aim to create the special structure for IN by de-interleaving in order to use the knowledge in (11) and (12).

Note r as one received OFDM symbol and $r^{'}$ as the de-interleaved OFDM symbol in the time domain. The process of de-interleaving can be described as

$$r^{'}(n) = r(M \times mod(n/J) + floor(n/J)), \quad (13)$$

where $0 \le n \le N - 1$, $mod()$ is remainder operator, $floor()$ rounds the input value to the nearest integer less than or equal to it. M is the interleaving interval and $N = JM$ as presented in the previous subsection. Imagine that IN bursts occur in the time domain, interleaving is applied to create several similar structures as presented in row vector x^α with different α, and thus interleaved IN can be regarded as superposition of them.

To clearly elaborate IN interleaving, it will be explained with two detailed cases. The parameters involved in these cases will also be used in the following sections for verification. In one OFDM symbol, $N = 512$ samples are adopted in the time domain and $N = 512$ subcarriers are also adopted. Interleaving interval $M = 16$ is used, and thus $J = N/M = 32$. All the parameter notations are consistent in the whole paper. In the following descriptions of interleaving, the desired signal at the receiver is ignored, because IN will be estimated based on null subcarriers without any information of the transmitted signal.

$$x^\alpha = \Big[\underbrace{0 \ \cdots \ 0}_{\alpha} \ \ \tilde{x}_0^\alpha \ \ \underbrace{0 \ \cdots \ 0}_{M^{'}} \ \ \tilde{x}_1^\alpha \ \ \cdots \ \ \underbrace{0 \ \cdots \ 0}_{M^{'}} \ \ \tilde{x}_{J-1}^\alpha \ \ \underbrace{0 \ \cdots \ 0}_{M^{'}-\alpha} \Big] \quad (9)$$

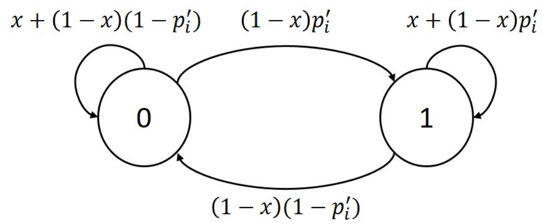

Fig. 2. a hidden Markov BG model with two terms.

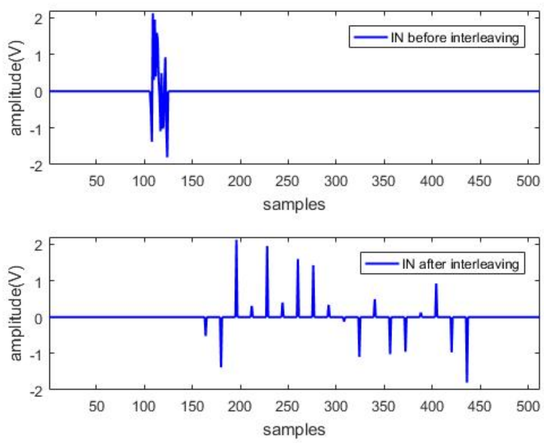

Fig. 3. Interleaved IN in case I.

1) Case I: In case I, IN is interleaved and displayed as one sequence structure like x^{α}, as shown in Fig. 3. Consequently, any two segments in the frequency domain satisfy the relationship shown in (12). If α is determined, given one segment, all the other segments can be obtained successively. Finally, IN after interleaving can be derived in the time domain by inverse FFT.

2) Case II: In case II, IN is interleaved as superpositions of 2 sequence structures like x^{α}, as presented in Fig. 4. The interleaved IN in Fig. 4 is expressed as x, and can be viewed as the summation of x^{α_1} and x^{α_2}, presented on the right side in Fig. 4, where α_1 and α_2 represent the numbers of zero at the start of two interleaved IN sequences.

$$x(n) = x^{\alpha_1}(n) + x^{\alpha_2}(n), \tag{14}$$

where $0 \leq n \leq N-1$. According to (11), both x^{α_1} and x^{α_2} have similar relationship between each two segments in the frequency domain as x^{α}. The FFT of x can be expressed as

$$X(k) = X^{\alpha_1}(k) + X^{\alpha_2}(k), \tag{15}$$

where $0 \leq k \leq N-1$. In light of (12), any two segments in the frequency domain are subject to

$$\begin{aligned} X(\tilde{m}_1) =& X^{\alpha_1}(\tilde{m}_1) + X^{\alpha_2}(\tilde{m}_1) \\ X(\tilde{m}_2) =& X^{\alpha_1}(\tilde{m}_2) + X^{\alpha_2}(\tilde{m}_2) \\ =& X^{\alpha_1}(\tilde{m}_1)e^{-i\frac{2\pi(\tilde{m}_2-\tilde{m}_1)\alpha_1}{M}} + X^{\alpha_2}(\tilde{m}_1)e^{-i\frac{2\pi(\tilde{m}_2-\tilde{m}_1)\alpha_2}{M}} \end{aligned} \tag{16}$$

where $0 \leq \tilde{m}_1, \tilde{m}_2 \leq M-1$.

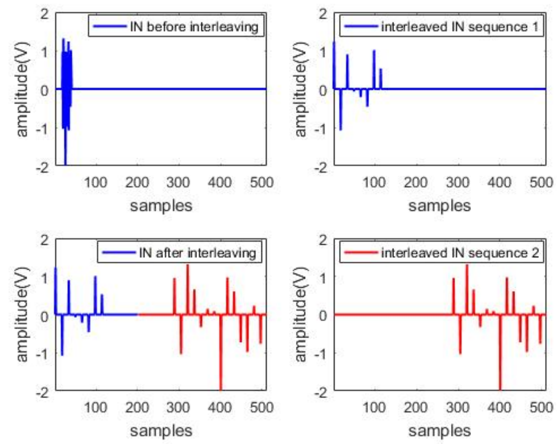

Fig. 4. Interleaved IN in case II.

In case II, if at least two segments of X, α_1 and α_2 are provided, the two corresponding segments of X^{α_1} and X^{α_2} can be recovered based on (16), thus two interleaved IN sequences can be recovered in time domain respectively.

Similarly, when IN occurrence is high or with longer time duration in the time domain, the interleaved IN can be viewed as the summation of more than two interleaved IN sequences described above. In these cases, they are still subject to the relationships described above.

Since IN bursts are interleaved and can be seen as the superposition of several sequences as x^{α}, each sequence as x^{α} after interleaving with IN will be called as IN interleaved sequence in the following sections.

IV. Noise Mitigation Based on MUSIC

In OFDM PLC systems, null subcarriers are reserved and can be used for IN estimation because they only include noise information. Noise mitigation based on MUSIC attempts to recover IN from the information on null subcarreirs. According to Homeplug AV and IEEE 1901, unused or null subcarriers are distributed in blocks or segments in the whole frequency band. In Section III B, we described the strong relationship between any two segments of the interleaved IN sequences in the frequency domain. Thus, the null subcarrier blocks represent the segments of the special structure described above, and we shall exploit them to estimate IN. However, we have no knowledge of the parameter α related to each IN interleaved sequence. Therefore, the first task is to estimate α. With FFT points N, and interleaving interval M, we can obtain M segments in the frequency domain, and each couple of segments have the relationship discussed in the two cases in the last section. Now let us assume that the first S segments of all M segments in the frequency domain act as null subcarriers. The interleaved received signal r' can be regarded as superpositions of M sequences as x^{α}, with $0 \leq \alpha \leq M-1$. In light of (11), the interleaved received

This article has been accepted for publication in a future issue of this journal, but has not been fully edited. Content may change prior to final publication. Citation information: DOI 10.1109/TSG.2018.2831913, IEEE Transactions on Smart Grid

signal in the frequency domain can be expressed as

$$\begin{aligned} R^{'}(J\tilde{m}+\tilde{j}) &= \sum_{\alpha=0}^{M-1} X^{\alpha}(J\tilde{m}+\tilde{j}) \\ &= \sum_{\alpha=0}^{M-1} \tilde{X^{\alpha}}(\tilde{j}) e^{-i\frac{2\pi\tilde{j}\alpha}{N}} e^{-i\frac{2\pi\tilde{m}\alpha}{M}}, \end{aligned} \tag{17}$$

where $R^{'}$ represents the FFT of the interleaved received signal $r^{'}$. If $\tilde{j}$ remains unchanged, the $\tilde{j}$th element in each segment can be rewritten in matrix form in (23). MUSIC is usually used for frequency estimation in wireless communication, where an antenna array is used to capture multiple signals with S directions of arrival (DOA). Compared to wireless communication, in our case, matrix B of size $S \times M$ in (23) can be seen as the phase delay caused by the antenna array, and $X(\tilde{j})$ in (23) can be seen as the collected signal vector by antenna arrary at timing $\tilde{j}$, where $\tilde{j}$ varies from 0 to $J-1$. In fact, there are only p signal sources for detection. In our cases, p signal sources are equal to p interleaved IN sequences. Therefore, MUSIC is applied to estimate α of each interleaved IN sequence. Our discussion is also subject to the condition that $S > p$.

A. Covariance Matrix Eigenvalue Decomposition (ED)

When $\tilde{j}$ is fixed, $R^{'}(\tilde{j})$ in (23) can be seen as all the collected signals on S antenna at timing $\tilde{j}$. The covariance of the interleaved received signal at timing $\tilde{j}$ will be calculated as

$$C_{RR}(\tilde{j}) = BX(\tilde{j})X(\tilde{j})^H B^H = BC_{XX}(\tilde{j})B^H, \tag{18}$$

where $C_{XX}(\tilde{j}) = X(\tilde{j})X(\tilde{j})^H$ in (24) and $()^H$ denotes Hermitian operator. The expectation of C_{RR} can be estimated as

$$E\{C_{RR}\} = \frac{1}{J}\sum_{\tilde{j}=0}^{J-1} C_{RR}(\tilde{j}) = \frac{1}{J}B\left(\sum_{\tilde{j}=0}^{J-1} C_{XX}(\tilde{j})\right)B^H, \tag{19}$$

where $E\{C_{XX}\} = \frac{1}{J}\sum_{\tilde{j}=0}^{J-1} C_{XX}(\tilde{j})$, and thus it is rewritten as

$$E\{C_{RR}\} = BE\{C_{XX}\}B^H. \tag{20}$$

The eigenvalues of $E\{C_{RR}\}$ are equal to those of $E\{C_{XX}\}$, as matrix B is a full rank matrix. After IN interleaving, the frequency spectrum of these interleaved IN sequences can be assumed to be independent, thus deriving

$$C_{XX}(\tilde{j}) = \begin{bmatrix} \left|\tilde{X^0}(\tilde{j})\right|^2 & 0 & 0 & 0 \\ 0 & \left|\tilde{X^1}(\tilde{j})\right|^2 & 0 & 0 \\ \cdots & \cdots & \cdots & \cdots \\ 0 & 0 & \cdots & \left|\tilde{X}^{M-1}(\tilde{j})\right|^2 \end{bmatrix}. \tag{21}$$

according to (24). Therefore, $E\{C_{XX}\}$ can be expressed as

$$E\{C_{XX}\} = \begin{bmatrix} \delta_0^2 & 0 & 0 & 0 \\ 0 & \delta_1^2 & 0 & 0 \\ \cdots & \cdots & \cdots & \cdots \\ 0 & 0 & \cdots & \delta_{M-1}^2 \end{bmatrix}, \tag{22}$$

where δ_α^2 is the variance related to the corresponding sequence $\tilde{x^\alpha}$ of αth interleaved sequence x^α in the time domain, and $0 \le \alpha \le M-1$.

After IN interleaving in the time domain, there will be several interleaved IN sequences. Let us assume that there are p interleaved IN sequences, and p is less than M. Considering background noise, most of the diagonal elements are equal to background noise variance, while only the diagonal elements corresponding to IN interleaved sequences are relatively high, representing the sum of the average power of the IN interleaved sequence and background noise. Here we give an empirical threshold of 2 for selecting the main eigenvalues, differentiating from those of background noise. It implies that if the averaged power of interleaved sequence is higher than twice the power of background noise, it is detected as an IN interleaved sequence. The estimated number of all the selected IN interleaved sequences is marked as $\hat{p}$. We select the $\hat{p}$ eigenvectors corresponding to the $\hat{p}$ selected eigenvalues to form the subspace matrix S_{IN}. The estimation of $\hat{p}$ was discussed theoretically [32], while it doesn't perform well in our case because of fewer samples for estimation. Therefore, an empirical threshold is adopted based on statistics, which will be discussed in the simulation. In this step, we only determine the number of IN interleaved sequence and its

$$R^{'}(\tilde{j}) = \begin{bmatrix} R^{'}(\tilde{j}) \\ R^{'}(J+\tilde{j}) \\ \cdots \\ R^{'}(J(S-1)+\tilde{j}) \end{bmatrix} = \begin{bmatrix} 1 & 1 & \cdots & 1 \\ 1 & e^{-i\frac{2\pi}{M}} & \cdots & e^{-i\frac{2\pi(M-1)}{M}} \\ \cdots & \cdots & \cdots & \cdots \\ 1 & e^{-i\frac{2\pi(S-1)}{M}} & \cdots & e^{-i\frac{2\pi(S-1)(M-1)}{M}} \end{bmatrix} \begin{bmatrix} \tilde{X^0}(\tilde{j})e^{-i\frac{2\pi\tilde{j}*0}{N}} \\ \tilde{X^1}(\tilde{j})e^{-i\frac{2\pi\tilde{j}*1}{N}} \\ \cdots \\ \tilde{X}^{M-1}(\tilde{j})e^{-i\frac{2\pi\tilde{j}*(M-1)}{N}} \end{bmatrix} = BX(\tilde{j}) \tag{23}$$

$$C_{XX}(\tilde{j}) = \begin{bmatrix} \tilde{X^0}(\tilde{j})e^{-i\frac{2\pi\tilde{j}*0}{N}} \\ \tilde{X^1}(\tilde{j})e^{-i\frac{2\pi\tilde{j}*1}{N}} \\ \cdots \\ \tilde{X}^{M-1}(\tilde{j})e^{-i\frac{2\pi\tilde{j}*(M-1)}{N}} \end{bmatrix} \begin{bmatrix} \tilde{X^0}(\tilde{j})e^{i\frac{2\pi\tilde{j}*0}{N}} & \tilde{X^1}(\tilde{j})e^{i\frac{2\pi\tilde{j}*1}{N}} & \cdots & \tilde{X}^{M-1}(\tilde{j})e^{i\frac{2\pi\tilde{j}*(M-1)}{N}} \end{bmatrix} \tag{24}$$

This article has been accepted for publication in a future issue of this journal, but has not been fully edited. Content may change prior to final publication. Citation information: DOI 10.1109/TSG.2018.2831913, IEEE Transactions on Smart Grid

projection space in the frequency domain. Next, we need to determine the concrete locations of these sequences.

B. Frequency Estimation (α Estimation)

In MUSIC method, frequency estimation is required to select the p DOA corresponding to the p transmitted signals, with the target that the interferences caused by other signals on each DOA should be minimum. In our case, the IN projection of each IN interlaved sequence onto time domain with the obtained subspace suffers from minimal interferences from others. The frequency estimation function can be expressed in (25). Since the number of IN interleaved sequences has been determined as $\hat{p}$, α values corresponding to the $\hat{p}$ largest function values will be detected, and the detected α values are denoted as vector $\hat{\alpha}$ of length $\hat{p}$. Therefore, the corresponding locations of all detected IN interleaved sequences will contribute to the IN support.

$$f(\alpha) = \frac{1}{B(\alpha)^H (I - S_{IN} S_{IN}^H) B(\alpha)}, \quad (25)$$

where $B(\alpha)$ refers to the αth column of matrix B, and $0 \leq \alpha \leq M-1$.

C. IN- estimation based on Least Squares

According to the former discussion, once all the α values of $\hat{p}$ IN interleaved sequences are selected as vector $\hat{\alpha}$, (23) can be reduced as

$$R^{'}(\tilde{j}) = B_{\hat{p}} X_{\hat{p}}(\tilde{j}), \quad (26)$$

where $B_{\hat{p}}$ is a submatrix of B, and all its columns are selected from matrix B, corresponding to the all $\hat{p}$ elements of vector $\hat{\alpha}$. Similarly, $X_{\hat{p}}(\tilde{j})$ refers to the subarray of $X(\tilde{j})$, corresponding to all $\hat{p}$ elements of vector $\hat{\alpha}$. $X_{\hat{p}}(\tilde{j})$ can be solved using LS method as

$$X_{\hat{p}}(\tilde{j}) = (B_{\hat{p}}^H B_{\hat{p}})^{-1} B_{\hat{p}}^H R^{'}(\tilde{j}), \quad (27)$$

where $0 \leq \tilde{j} \leq J-1$. Since all the elements of $X_{\hat{p}}(\tilde{j})$ are recovered, we can deduce $\tilde{X}^{\alpha}$ with each estimated element in $\hat{\alpha}$. Therefore, each IN interleaved sequence is recovered in the time domain by inverse FFT of $\tilde{X}^{\alpha}$.

V. SPARSE BAYESIAN LEARNING WITH MUSIC

SBL is used for sparse signal recovery. (7) is a linear regression problem, in which R_{null} is an observation vector F_{null} is an overcomplete basis, and i, denoting IN in the time domain, is a sparse weight vector to be estimated. SBL impose a parameterized Gaussian prior on i,

$$p(i, \Gamma_i) = N(i; 0; \Gamma_i), \quad (28)$$

where Γ_i represents the diagonal matrix of i with $\Gamma_i = diag\{\gamma\}$, and γ_i is a vector whose nth element γ_n is the variance of i_n. Maximum likelihood (ML) estimator is used to calculate the hyperparameter γ using expectation maximization (EM), and maximum a posteriori (MAP) estimate of IN $\hat{i}$ is obtained with its distribution of $N(\hat{i}; \mu_i, \Sigma_i)$. In the process of iterations, the support of i is initialized to be full, and matrix operations involved in updating Σ_i are implemented in full size. Then the support is updated in each iteration by pruning γ, and all the computation in size will be reduced subsequently.

TABLE I

Input: Sampling matrix F_{null}, Observed vector R_{null}, Candidate support list $List_{IN}$ based on MUSIC;
Output: IN Approximation $\hat{i}$

Initialization
$diag(\Gamma)(List_{IN}) = 1$, $\mu_i = 0$, $\Sigma_i = 0$;
$k = 1$ iteration index
repeat
  1. prune γ and associated components in Σ_i
  2. construct new F_{null} corresponding to new γ_k
  3. calculate new weights
    $\mu_i^{k+1} = (\delta_w^{-2})^k \Sigma_i^k F_{null}^H R_{null}$
    $\Sigma_i^{k+1} = ((\delta_w^{-2})^k F_{null}^H F_{null} + (\Gamma^k)^{-1})^{-1}$
  4. estimate γ
    $\gamma_i^k = \Sigma_{i,nn}^k + (\mu_{i,n}^k)^2$
  if halting condition true that
  quit the iteration;
  else $k = k + 1$
  end if
until halting condition true;
Output: $\hat{i} = \mu_i$

As discussed in last section, the candidate support of IN can be determined based on MUSIC. Therefore, we combine MUSIC and SBL algorithms together to reduce the computation overhead. Besides, this also improves its performance with a more accurate estimation. In MUSIC support estimation, there is a condition that the number of S segments should be larger than the p interleaved IN sequences. Prior knowledge of the IN width can be used generally, however we don't know the width in advance for estimating the number of S to be used. Besides, it is also supposed that all the subcarriers of S segments are used as null subcarriers, since it is required for noise estimation in LS. In summary, with fewer segments or fewer elements in each segment, the accuracy of IN support estimation will be decreased. Therefore, we expand the IN candidate support by a factor of 2, based on frequency estimation function. For example, if the primary estimation of p is $p1$, we select the first $2 \times p1$ α values corresponding to the $2 \times p1$ largest estimation function values. If one OFDM symbol suffers from less IN interference, the primary $p1$ is estimated to be smaller and more accurately. Correspondingly, we only select its twice size as candidate support size. Conversely, when IN interference is heavy, the primary estimation of $p1$ is estimated to be larger and less accurately. IN estimation support is enlarged to be two times of its original size, so that all the real IN supports are not missed.

The iteration steps of SBL are shown in Tab.I. In the iteration steps, δ_w^2 represents the variance of background noise, and remains fixed in the iteration, because it can be estimated at receiver generally. It helps to reduce much computation overhead without updating δ_w^2. $\Sigma_{i,nn}$ represents the (n,n)th element in matrix Σ_i, and $\mu_{i,n}$ represents the nth element in vector μ_i. $diag()$ selects the diagonal elements of a matrix.

VI. SIMULATION

According to Homeplug AV and IEEE 1901, unused or null subcarriers are distributed in blocks or segments in the whole frequency band. As a matter of fact, the null subcarrier blocks are not necessarily consecutive in our method. In order to simplify the simulation, we assume that the unused subcarrier segments are consecutive in frequency band. In our simulation, an OFDM system with $N = 512$ subcarriers is assumed, in which the subsets of first 256 subcarriers act as null subcarriers and the remaining 256 subcarriers are used for signal transmission. To evaluate the proposed IN mitigation algorithms, a frequency flat channel is considered for all the subcarriers. Each subcarrier conveys complex symbols that are coded with QAM 4 modulation. In the PLC OFDM system, channel coding is not considered. As shown in Fig. 1, interleaving is adopted in the time domain at transmitter, while received signal is deinterleaved at receiver, which creates the special structure for IN simultaneously. IN will be mitigated from received signal with IN estimation at the receiver. The noise is modeled by a hidden Markov BG model with index parameter $A = 0.005$ and correlation parameter $x = 0.9$, and thus the transmission matrix is

$$T = \begin{bmatrix} 0.9995 & 0.0005 \\ 0.0995 & 0.9005 \end{bmatrix}.$$

In addition, Γ varies corresponding to INR ranging from 20dB to 40dB. Besides, the numbers of null subcarriers $[128, 160, 192, 224, 256]$ are also considered to validate the proposed method, and they are referred to as 25%, 31.25%, 37.5%, 43.75% and 50% of all the subcarriers. In addition, we applied three algorithms to evaluate the performance, including SBL, SBL with prior knowledge acquired from MUSIC, and MUSIC combined with LS.

In MUSIC algorithm discussed previously, the threshold of selecting the number of IN interleaved sequences is selected based on statistics. All the PDFs of correctly detecting IN interleaved sequences are presented in Fig.5 under different conditions that INR varies from 20dB to 40dB, and different numbers of null subcarriers are considered. It can be noted that 2 is the optimal threshold among the range of 1 to 4 in all conditions. The detection accuracy is improved with the increasing number of null subcarriers, since more information of IN is included.

Generally, it can be noted from Fig. 6-8 that the performance of each method improves with the increase of subcarriers because more information of IN are provided. In addition, SBL algorithm with MUSIC performs better than the other two methods with different INRs, because it combines the advantages of the two methods. As presented in Fig. 6, MUSIC with SBL achieves about 5dB gain at bit error rate (BER) level of 10^{-4} with 43.75% subcarriers, while SBL achieves 3dB gain, even though MUSIC with LS shows rather poor performance. In Fig. 8, both MUSIC with SBL and MUSIC with LS perform much better than SBL with 50% subcarriers, achieving 10dB and 7dB more than SBL does, respectively. It can be seen that even though either SBL or MUSIC with LS performs poorly, MUSIC with SBL still keeps an advantage over any of them.

With the increase of INR, it can be observed that all of these methods perform better, achieving a higher gain than the conventional system without any IN mitigation techniques. In all of these algorithms, background noise can be viewed as inference for IN recovery, while IN is the desired signal to be estimated. Obviously, it would be easier to recover IN with a high INR. Actually, INR is defined in the time domain, and IN only occurs with low probability, leading to the fact that the averaged power of INR on each null subcarrier is lower than the so-called INR. Therefore, when INR is equal to 20dB as presented in Fig. 6, all the methods achieve lower gain, compared with INR equal to 30dB and 40dB, as presented in Fig. 7-8.

When INR are 30dB and 40dB, MUSIC with LS method performs similarly with SBL basically, and even better with more subcarriers, as displayed in Fig. 7-8. However, as shown in Fig. 6, it performs poorly when SNR increases with less than 50% subcarriers. This can be explained as IN fails to be estimated accurately with insufficient information, and the performance is further degraded with badly estimated IN support with fewer subcarriers. It implies that MUSIC with LS method is not robust to IN bursts with high width.

The previous simulations are conducted with the ideal frequency flat channel assumption. However, power line channels are frequency selective fading due to multiple branches in power line networks. According to [33], a four-path model in the frequency domain is adopted with all the provided parameters. The channel transfer function is presented in Fig.9 with the sampling frequency of 20MHz and the subcarrier bandwidth of 25 kHz that is close to the subcarrier bandwidth of 24.414 kHz defined in IEEE 1901. MMSE channel equalizer is used at the receiver. Similarly, the proposed method is examined with different percentage occupations of all the subcarriers varying from 25% to 50%, and INR varying from 20dB to 40dB. The results are presented in Fig.10-12, and SNR is referred to as the ratio of the power of the ideal transmitted signal to the power of background noise. As the results in the case of ideal channel assumption presented in Fig.6-8, the performances of the three methods improve with respect to the conventional method with the increase of INR and subcarriers. When SNR is below a certain value such as 25dB in the simulation with frequency selective fading channel, MUSIC with LS performs slightly better than SBL. This offers a slight advantage to the method of MUSIC with SBL. With the increase of SNR, the performance of MUSIC with LS becomes worse than SBL gradually, and thus the advantage of SBL combined with MUSIC provided by MUSIC disappears and the performances of SBL and MUSIC with SBL become similar.

With regard to the computation cost, MUSIC with LS and MUSIC with SBL are implemented with less time overhead than SBL algorithms due to matrix inverse operation of large size in each iteration in SBL alogrithm. For example, all the computations are conducted in MATLAB with i5-6600 CPU. SBL algorithm costs 2.21s with 50% subcarriers to estimate IN, while MUSIC with SBL costs 0.59s, because the reduced support of IN gives rise to matrix operation of smaller size. MUSIC with LS costs only 9×10^{-3}s.

This article has been accepted for publication in a future issue of this journal, but has not been fully edited. Content may change prior to final publication. Citation information: DOI 10.1109/TSG.2018.2831913, IEEE Transactions on Smart Grid

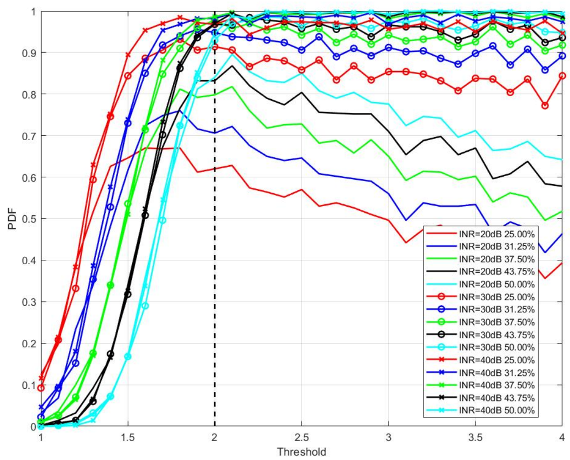

Fig. 5. PDF of IN sequence correct detection versus threshold

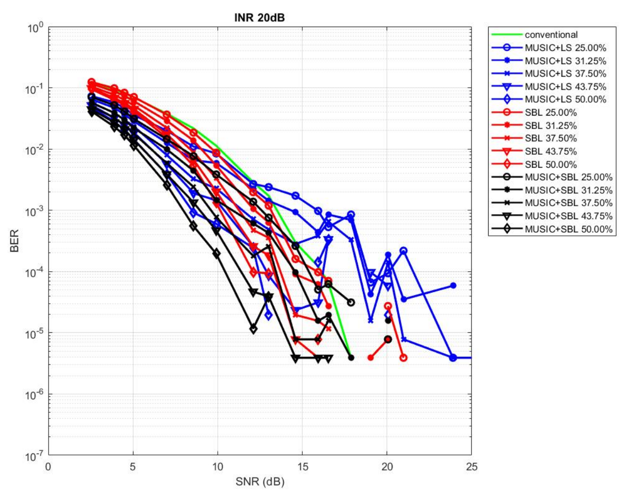

Fig. 6. BER comparison of INR=20dB

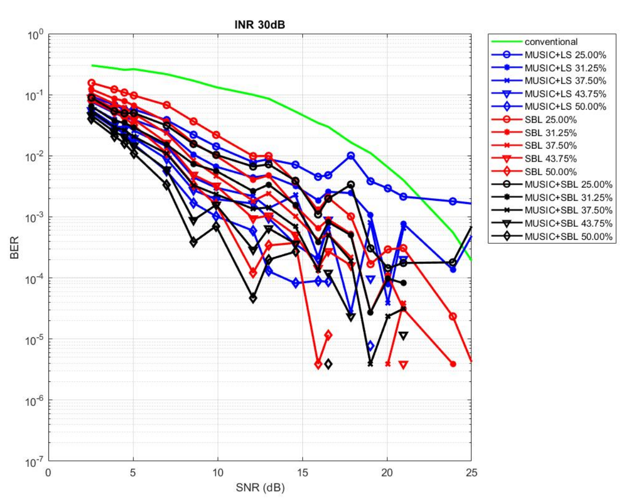

Fig. 7. BER comparison of INR=30dB

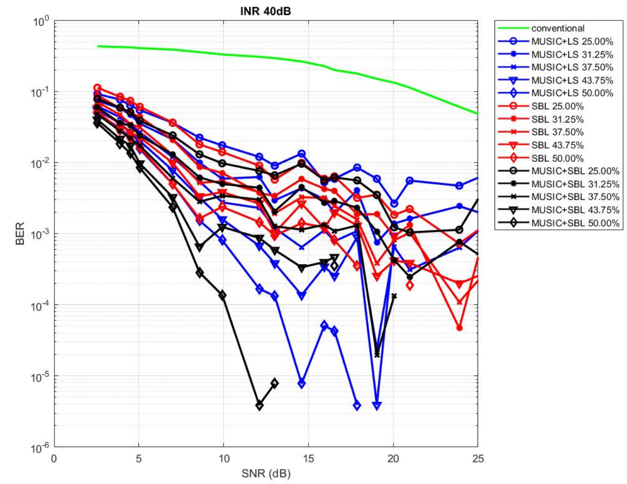

Fig. 8. BER comparison of INR=40dB

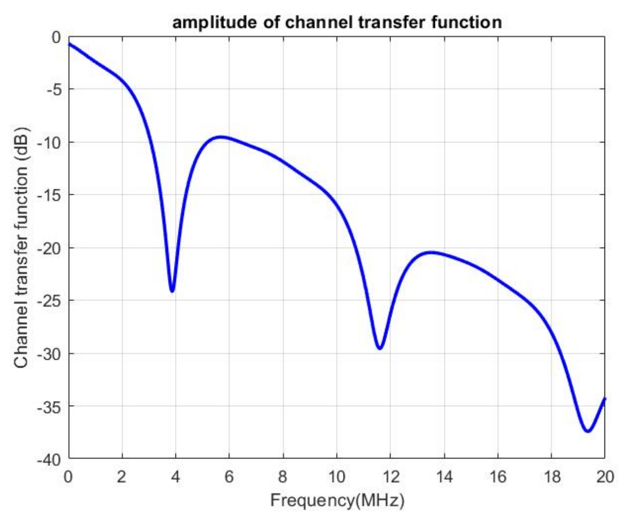

Fig. 9. Amplitude response of channel transfer function

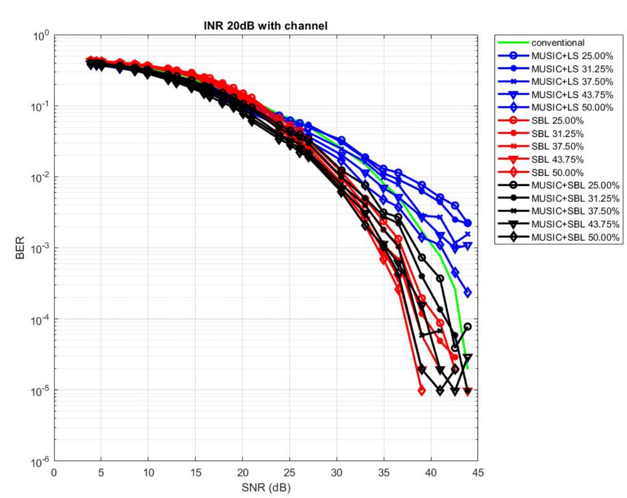

Fig. 10. BER comparison of INR=20dB with channel

This article has been accepted for publication in a future issue of this journal, but has not been fully edited. Content may change prior to final publication. Citation information: DOI 10.1109/TSG.2018.2831913, IEEE Transactions on Smart Grid

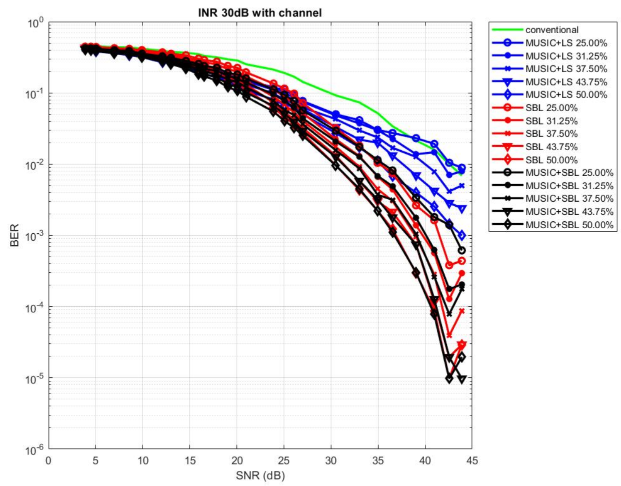

Fig. 11. BER comparison of INR=30dB with channel

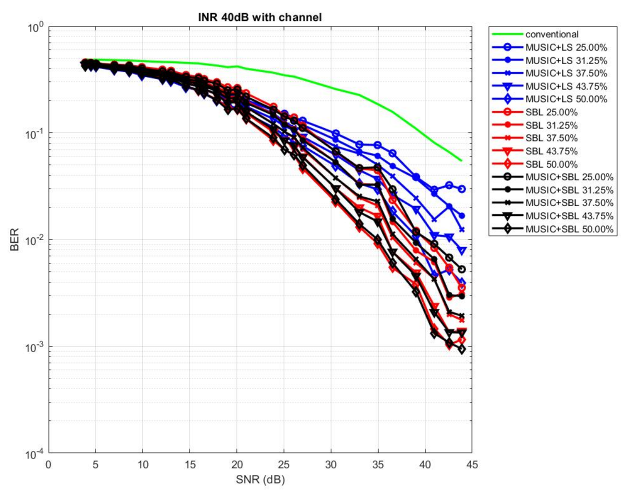

Fig. 12. BER comparison of INR=40dB with channel

VII. Conclusion

In this paper, IN mitigation with interleaving based on MUSIC is proposed for IN support detection based on time domain interleaving, with IN bursts assumption. The LS algorithm is applied for IN estimation in the frequency domain. Besides, MUSIC with SBL based IN support detection is also investigated. The proposed MUSIC with LS method performs closely to SBL with higher INRs, while its performance degrades because of inaccurate IN support estimation with lower INR. Moreover, MUSIC with SBL holds advantages of MUSIC with LS algorithm and SBL method, performing best among three methods. It is also implemented with less computation overhead compared with SBL algorithm.

Acknowledgment

This work was supported by the University of Pisa under the PRA Progetti di Ricerca di Ateneo, grant number PRA_2017_33.

References

[1] L. T. Berger, A. Schwager, and J. J. Escudero-Garzs, "Power Line Communications for Smart Grid Applications, *JECE,* vol. 2013, pp. 1-16, 2013.

[2] D. Anastasiadou and T. Antonakopoulos, "Multipath characterization of indoor power-line networks," *IEEE Trans. Power Del.,* vol. 20, no. 1, pp. 90-99, Jan. 2005.

[3] J. A. Cortes, L. Diez, F. J. Canete and J. J. Sanchez-Martinez, "Analysis of the Indoor Broadband Power-Line Noise Scenario," *IEEE Trans. Electromagn. Compat.,* vol. 52, no. 4, pp. 849-858, Nov. 2010.

[4] M. Zimmermann and K. Dostert, "Analysis and modeling of impulsive noise in broad-band powerline communications," *IEEE Trans. Electromagn. Compat.,* vol. 44, no. 1, pp. 249-258, Feb. 2002

[5] V. Degardin, M. Lienard, A. Zeddam, F. Gauthier and P. Degauquel, "Classification and characterization of impulsive noise on indoor powerline used for data communications," *IEEE Trans. Consum. Electron.,* vol. 48, no. 4, pp. 913-918, Nov 2002.

[6] Al-Dweik, A.; Hazmi, A.; Sharif, B. and Tsimenidis, C., "Efficient interleaving technique for OFDM system over impulsive noise channels," *21st Annu. IEEE Int. Symp. Personal, Indoor and Mobile Radio Communications,* Instanbul, 2010, pp. 167-171.

[7] S. Nayyef, C. Tsimenidis, A. Al-Dweik, B. Sharif and A. Hazmi, "Time- and Frequency-Domain Impulsive Noise Spreader for OFDM Systems," *11th Int. Conf. Trust, Security and Privacy in Computing and Communications,* Liverpool, 2012, pp. 1856-1861.

[8] S. Liu, F. Yang and J. Song, "An Optimal Interleaving Scheme With Maximum Time-Frequency Diversity for PLC Systems," *IEEE Trans. Power Del.,* vol. 31, no. 3, pp. 1007-1014, June 2016.

[9] K. S. Al-Mawali and Z. M. Hussain, "Performance of bit-interleaved coded OFDM in power line communications with impulsive noise," *Int. Conf. Advanced Technologies for Communications,* Hai Phong, 2009, pp. 49-53.

[10] N. Andreadou and A. M. Tonello, "On the Mitigation of Impulsive Noise in Power-Line Communications With LT Codes," *IEEE Trans. Power Del.*, vol. 28, no. 3, pp. 1483-1490, July 2013.

[11] T. Shongwe, A. J. H. Vinck and H. C. Ferreira, "The effects of periodic impulsive noise on OFDM," *IEEE Int. Symp. Power Line Communications and Its Applications,* Austin, TX, 2015, pp. 189-194.

[12] S. V. Zhidkov, "Analysis and comparison of several simple impulsive noise mitigation schemes for OFDM receivers," *IEEE Trans. on Commun.,* vol. 56, no. 1, pp. 5-9, Jan. 2008.

[13] S. V. Zhidkov, "Performance analysis and optimization of OFDM receiver with blanking nonlinearity in impulsive noise environment," *IEEE Trans. Veh. Technol.,* vol. 55, no. 1, pp. 234-242, Jan. 2006.

[14] K. S. Al-Mawali and Z. M. Hussain, "Adaptive-threshold clipping for impulsive noise reduction in OFDM-based power line Communications," *Int. Conf. Advanced Technologies for Communications,* Hai Phong, 2009, pp. 43-48.

[15] G. Ndo, P. Siohan and M. H. Hamon, "Adaptive Noise Mitigation in Impulsive Environment: Application to Power-Line Communications," *IEEE Trans. Power Del.,* vol. 25, no. 2, pp. 647-656, Apr. 2010.

[16] U. Epple and M. Schnell, "Adaptive threshold optimization for a blanking nonlinearity in OFDM receivers," *IEEE Global Communications Conf.,* Anaheim, CA, 2012, pp. 3661-3666.

[17] F. H. Juwono, Q. Guo, Y. Chen, L. Xu, D. D. Huang, and K. P. Wong, "Linear combining of nonlinear preprocessors for OFDM-based powerline communications," *IEEE Trans. Smart Grid,* vol. 7, no. 1, pp. 253-260, Jan. 2016.

[18] F. H. Juwono, Q. Guo, Y. Chen, L. Xu, D. D. Huang, and K. P. Wong, "On the performance of blanking nonlinearity in real-valued OFDM-based PLC," *IEEE Trans. Smart Grid,* vol. PP, 2017.

[19] K. M. Rabie and E. Alsusa, "Quantized Peak-Based Impulsive Noise Blanking in Power-Line Communications," *IEEE Trans. Power Del.,* vol. 29, no. 4, pp. 1630-1638, Aug. 2014.

[20] K. M. Rabie, E. Alsusa, A. D. Familua and L. Cheng, "Constant envelope OFDM transmission over impulsive noise power-line communication channels," *IEEE Int. Symp. on Power Line Communications and Its Applications,* Austin, TX, 2015, pp. 13-18.

[21] A. Mehboob, L. Zhang and J. Khangosstar, "Adaptive impulsive noise mitigation using Multi Mode Compressive Sensing for powerline communications," *IEEE Int. Symp. on Power Line Communications and Its Applications,* Beijing, 2012, pp. 368-373.

[22] G. Caire, T. Y. Al-Naffouri and A. K. Narayanan, "Impulse noise cancellation in OFDM: an application of compressed sensing," *IEEE Int. Symp.on Information Theory,* Toronto, ON, 2008, pp. 1293-1297.

[23] G. Ren, S. Qiao and Y. Hei, "Asynchronous impulsive noise mitigation in OFDM using adaptive threshold compressive sensing,", *IEEE Ann. Wireless and Microwave Technology Conf.,* Tampa, FL, 2014, pp. 1-5.

[24] S. Liu, F. Yang, W. Ding and J. Song, "Double kill: Compressive-sensing-based narrow-band interference and impulsive noise mitigation for vehicular communications," *IEEE Transactions on Veh. Technol.,* vol. 65, no. 7, pp. 5099-5109, Jul. 2016.

[25] J. Lin, M. Nassar and B. L. Evans, "Impulsive Noise Mitigation in Powerline Communications Using Sparse Bayesian Learning," *IEEE J. Sel. Areas Commun.,* vol. 31, no. 7, pp. 1172-1183, Jul. 2013.

[26] J. Lin and B. L. Evans, "Non-parametric mitigation of periodic impulsive noise in narrowband powerline communications," *IEEE Global Communications Conf.,* Atlanta, GA, 2013, pp. 2981-2986.

[27] T. Y. Al-Naffouri, A. A. Quadeer and G. Caire, "Impulse Noise Estimation and Removal for OFDM Systems," *IEEE Trans. Commun.,* vol. 62, no. 3, pp. 976-989, Mar. 2014.

[28] D. Shrestha, A. Tonello, X. Mestre and M. Payar, "Simultaneous cancellation of narrow band interference and impulsive noise in PLC systems," *IEEE Int. Conf. Smart Grid Communications,* Sydney, NSW, 2016, pp. 326-331.

[29] D. Shrestha, X. Mestre and M. Payar, "Asynchronous impulsive noise mitigation based on subspace support estimation for PLC systems," *Int. Symp. Power Line Commun. and its Applica.,* Bottrop, 2016, pp. 1-6.

[30] H. Mohimani, M. Babaie-Zadeh, I. Gorodnitsky and C. Jutten et al. "Sparse recovery using smoothed l0 (sl0): Convergence analysis, *IEEE Trans. Inf. Theory.*, vol. abs-1001-5073, Jan. 2010.

[31] G. Ndo, F. Labeau and M. Kassouf, "A Markov-Middleton Model for Bursty Impulsive Noise: Modeling and Receiver Design," *IEEE Trans. on Power Del.,* vol. 28, no. 4, pp. 2317-2325, Oct. 2013.

[32] M. Wax and T. Kailath, "Detection of signals by information theoretic criteria," *IEEE Transactions on Acoust., Speech, and Signal Processing,* vol. 33, no. 2, pp. 387-392, Apr. 1985.

[33] M. Zimmermann and K. Dostert, "A multipath model for the powerline channel," *IEEE Transactions on commun.*, vol. 50, no. 4, pp. 553-559, Aug. 2002.

Li Bai received the bachelor and master degree in electrical engineering from Xi'an Jiaotong University, Xi'an, China, in 2006 and 2009 respectively. She is pursuing Ph.D degree in electrical engineering in University of Pisa. Her research interests include power line communication and smart grid.

Mauro Tucci received the Ph.D. degree in applied electromagnetism from the University of Pisa, Pisa, Italy, in 2008. Currently, he is an Associate Professor with the Department of Energy, Systems, Territory and Constructions Engineering, University of Pisa. His research interests include computational intelligence and big data analysis, with applications in electromagnetism, non destructive testing, powerline communications, and smart grids.

Marco Raugi received the Ph.D. degree in electrical engineering from the University of Pisa, Pisa, Italy, in 1990. Currently, he is a Full Professor of Electrical Engineering with the Department of Energy, Systems, Territory and Constructions Engineering, University of Pisa. He is the author of many papers in international journals and conference proceedings. His research interests include numerical electromagnetics, with main applications in nondestructive testing, electromagnetic compatibility, communications, and computational intelligence. Prof. Raugi was the General Chairman of the international conferences Progress in Electromagnetic Research Symposium in 2004 and IEEE Symposium on Power Line Communications in 2007. He was the recipient of the IEEE Industry Application Society 2002 Melcher Prize Paper Award.